PNAS RESEARCH ARTICLE | CHEMISTRY

Pressure-induced redox reversal of iron and the distribution of elements in deep Earth

Q:1 Xiaoli Wang[a,1], Xiaolei Feng[b,1], Jianfu Li[a,1], Yang Lv[a], Austin Ellis[c], Samantha Scott[c], Abhiyan Pandit[c], Dalar Khodagholian[c],
Q:2 Russell J. Hemley[d,e,f], Matthew Jackson[g,2], Frank Spera[g], Simon Redfern[h,2], and Maosheng Miao[c,g,2]

Affiliations are included on p. 6.

Edited by Ho-kwang Mao, Chinese Academy of Sciences Shanghai Advanced Research Institute, Pudong, Shanghai, China; received July 25, 2024; accepted October 2, 2025

Q:9 **We demonstrate a remarkable change in the chemical bonding of iron under pressure that underlies the distribution of elements in the Earth's mantle and core. Using a massive-scale, first-principles study, we show that while reacting with *p*-block elements under increasing pressure from ambient to Earth core conditions, iron tends to reverse its redox nature, changing from an electron donor (reductant) to an electron acceptor (oxidant), and oxidizes many *p*-block elements. Such reverse redox propensity significantly impacts the stoichiometries, bond types and strengths, structures, and properties of iron compounds under deep planetary conditions. This change transforms many *p*-block elements (conventionally labeled lithophile or chalcophile) into highly siderophile species. The chemical binding strengths with iron show an inverse correlation with the depletion of *p*-block elements in the silicate Earth. Furthermore, silicon shows a distinct anomaly in its bonding to iron, which suggests silicon may readily be incorporated into Earth's core.**

high pressure | deep Earth | *p*-block elements | iron chemistry

Significance

The oxidation–reduction behavior of iron under pressure in part controls the chemical processes occurring in the deep Earth. Large-scale first-principles calculations show that iron reverses its redox nature under core pressures, shifting from an electron donor to an electron acceptor. This finding implies that many elements previously classified as lithophile or chalcophile could become siderophile under extreme conditions. This work challenges traditional models of elemental sequestration and introduces chemistries of iron that could explain the presence of light elements in the core and the observed anomalies in element depletion in the silicate Earth. The findings underscore the importance of considering high-pressure conditions in geochemical models and open pathways for exploring the composition and dynamics of Earth's interior. Q:6 Q:7 Q:8

The distribution and abundance of both major and trace elements in the Earth's interior provide a record of its formation and evolution (1, 2). An understanding of this record demands knowledge of the chemical affinity of the elements and their compounds under the high-pressure conditions of Earth's interior. For many years, our understanding of such affinities has been predominantly biased by low-pressure observations that are of dubious applicability to Earth's deep mantle and core (3). Many trace elements are found to have greatly reduced concentrations on Earth relative to their solar abundance (4, 5). This is usually explained in terms of either the escape of elements to space due to volatility during the high-energy conditions of terrestrial accretion (6), or the incorporation into the Earth's core (7). The core sequestration model relies on the reactivity of trace elements with Fe (and Ni) under high pressure, which is problematic to assess due to the difficulty of experimentally achieving terrestrial core pressures (135 to 367 GPa).

Thanks to improvements in computational power and methods, the high-pressure chemistry of Fe has become accessible, leading to the discovery of a number of new Fe compounds with trace elements that support the argument that they are incorporated in the core. For example, recent work showed that iron may actually bind strongly with xenon to form an Fe_3Xe compound at the pressures of Earth's core, suggesting that core sequestration is the cause of the "missing xenon paradox" (8, 9). A similar mechanism was suggested for the depletion of iodine in Earth (10), although the volatility of the xenon and iodine renders this explanation ambiguous. The reactions of Fe with major elements such as O also become quite unusual at very high pressure. As revealed by both computer simulation and diamond anvil cell experiments, iron can form an oxygen-rich FeO_2 compound at the pressures of Earth's lower mantle, even if it remains in the low oxidation state of +2 (11–13). We show here that these striking phenomena are all related to dramatic changes in "iron chemistry" under high pressure. The broad-ranging chemical trends of iron can only be revealed by a large-scale study of iron reactivity across the periodic table, a task that cannot be performed experimentally with reasonable resources and time.

Many recent studies show that first principles structure predictions are sufficiently advanced that enthalpies of compound formation at high pressure can be accurately calculated and the nature of the chemical bond elucidated (8–10, 13–18). Using this approach based on density functional theory (DFT), we have systematically explored the bonding of iron with *p*-block elements in the periodic table. The results indicate a fundamental shift in Fe chemistry at high pressures, where iron transitions from an electron donor to an electron acceptor, reversing its redox behavior. This redox reversal allows iron

The authors declare no competing interest.

This article is a PNAS Direct Submission.

[1]X.W., X.F., and J.L. contributed equally to this work.

[2]To whom correspondence may be addressed. Email: jackson@geol.ucsb.edu, simon.redfern@ntu.edu.sg, or mmiao@csun.edu.

Q:16 This article contains supporting information online at https://www.pnas.org/lookup/suppl/doi:10.1073/pnas.2414911122/-/DCSupplemental.

Published XXXX.

to strongly bond under pressure with many p-block elements that are conventionally labeled as lithophile or chalcophile (1, 19), making them highly siderophile. While compared with abundance data, the depletion of the p-block elements in the silicate Earth was found to correlate inversely with Fe binding strength. This striking result suggests that although the Earth's core can host large quantities of p-block elements, it is not the cause of their depletion. Instead, cosmochemical accretion models that call on elemental loss by volatility during high-energy conditions of terrestrial accretion may be more relevant (20). Furthermore, silicon shows a distinct anomaly in its bonding to iron, with the Fe–Si bond becoming one of the strongest at these high-pressure conditions. This result suggests that silicon may readily be incorporated into Earth's core, corroborating recent perspectives on the composition of Earth's core based on sound speed measurements, experimental petrology, and seismology (21, 22).

Results and Discussion

We conducted massive-scale first-principles simulations studying the reactivity of Fe with most of the p-block elements and its dependence on increasing pressure. For each element (X), the structures of a series of compositions (Fe_nX_m) are searched by Particle Swarm Optimization (PSO) algorithm (23) and density functional calculations. The p-block elements includes three major constituent elements S (1-bar boiling point of 721 K; 50% condensation temperature at 10^{-4} bar of 664 K), Si (2,628 K; 1,310 K), and P (556 K; 1,229 K) and a suite of geochemically trace elements such as Ge (3,103 K; 883 K), As (886 K; 1,065 K), Se (958 K; 697 K), Sn (2,543 K; 704 K), Sb (2,023 K; 979 K), and Te (1,263 K; 709 K) which are critical for understanding planetary accretion and core formation. Condensation temperatures are useful to consider when assessing whether a particular element is deficient in the silicate mantle relative to chondrites because it suffered volatilization and loss to space during planetary formation; it is a major task to explore whether such elemental deficiencies are due to volatile loss or relate instead to elements being "hidden" in the metallic core.

Iron Compound Stability and Elemental Abundances. Our calculations reveal that pressure can dramatically increase the stability of iron compounds formed with most p-block elements as evidenced by a significant decrease of formation enthalpy (Fig. 1). Although some $2p$ elements (e.g., C, N, O) can form stable compounds with iron with a ΔH_f of approximately −0.5 eV/atom at ambient conditions, a subset of $3p$ (e.g., Si, P, S; Fe—Al compounds are excepted, and will be discussed separately) and $4p$ (e.g., Ge, As, Se) elements bind only loosely with iron. This general trend of reactivity is markedly changed upon increasing

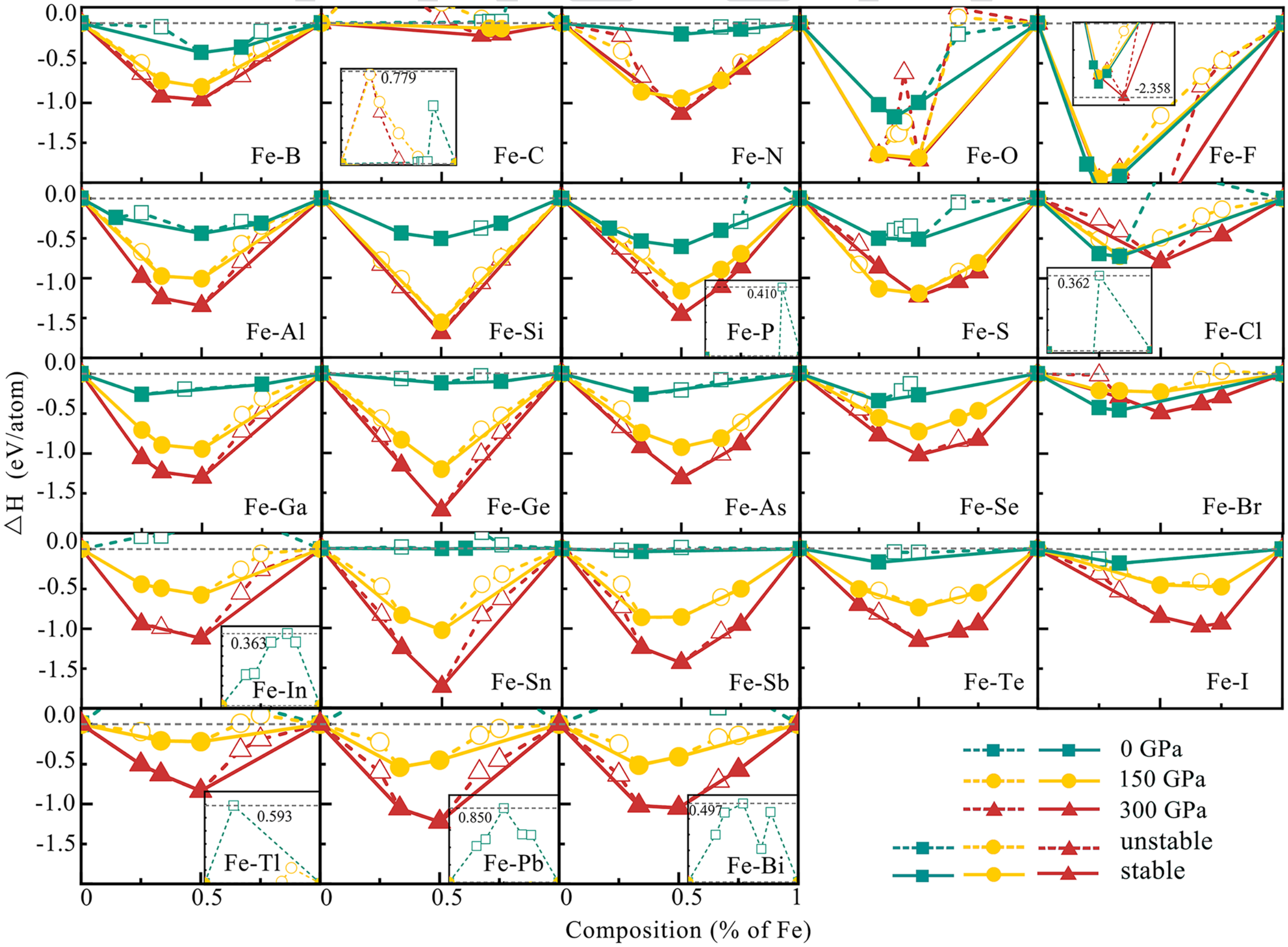

Fig. 1. Thermodynamic stability of main p-block—iron compounds at both ambient and high pressures. Most structures at ambient pressure are chosen from Materials Project (24). Most structures of Fe_mX_n (m/n = 1 to 3) at high pressures are obtained from crystal structure searches using PSO algorithm (23, 25) (details are shown in *Materials and Methods*). Convex hulls are shown as solid lines, with stable compounds shown by solid symbols. Unstable compounds (open symbols) sit above convex hulls, with dotted lines indicating possible decomposition routes.

 https://doi.org/10.1073/pnas.2414911122

pressure: Most of these elements can form stable compounds with iron with a ΔH_f of at least −1 eV/atom. For example, Fe and Te are not likely to form stable compounds with Fe (with $\Delta H_f = -0.2$ eV/atom) at 0 GPa. However, ΔH_f decreases by 1 eV/atom under high pressure, making the compound FeTe as stable as FeS at Earth-core pressures (e.g., 300 GPa).

Before discussing how these results impact our understanding of Earth chemistry, we examine the effects of temperature, electron correlation, and spin polarization. Both pressure and temperature increase with depth within the planet. To account for temperature effects, we calculated phonon free energies under the quasiharmonic approximation (QHA). While high temperatures shift formation free energies to varying degrees depending on the compound, they do not alter overall stability (*SI Appendix*, Fig. S1). As a 3d metal, Fe exhibits strong on-site electron–electron Coulomb interactions, especially at low pressures. These interactions are typically reduced under high pressure due to the delocalization of the electron states. However, previous studies have shown that correlations can still significantly influence the transport and thermochemical properties of Fe, even under Earth's core conditions (26, 27). A more recent study, using first-principles dynamic mean-field theory (DFT+DMFT) and a universal Hubbard U value of 5 eV and 10 eV, revealed that the time-dependent effect of correlation may alter the thermochemical properties of Fe–O compounds (28). Accurately accounting for the correlation effects across all Fe compounds in our study is challenging, even at the DFT+U level, as the appropriate U values can vary significantly depending on the compound type and pressure conditions. To systematically evaluate correlation effects, we performed DFT calculations using the Heyd–Scuseria–Ernzerhof (HSE) hybrid functional. The results indicate that the static effect of electron correlation has a negligible impact on the thermodynamic stability of Fe compounds across the 0 to 300 GPa pressure range (*SI Appendix*, Fig. S2). We also evaluated spin polarization at 0 GPa, as it is fully suppressed at 150 and 300 GPa. At low pressures, magnetism stabilizes Fe compounds with chalcogens and halogens by 0.2 to 0.5 eV/atom but does not affect the convexity of Fe–X systems (*SI Appendix*, Fig. S3). Our study primarily focuses on Fe compounds under high pressure, with low-pressure calculations included for comparison.

This pressure-enhanced Fe reactivity may promote the incorporation of many *p*-block elements, especially the heavier ones that were previously disregarded due to their weak or absent binding with Fe, into Earth's core. Like previous work (8–10), our results first appear to support core sequestration models; i.e., the depletion of certain elements in the silicate Earth arise from their incorporation into Earth's core. However, the integrated picture that compares the abundance of elements and their binding strength with Fe across the *p*-block of the periodic table shows the opposite trend. The *p*-block element abundances, normalized to CI chondrites, are *inversely* correlated with their binding strength to Fe as quantified by the formation enthalpies of the most stable compounds (Fig. 2 *A*–*C*); i.e., the stronger they bind with Fe the less they are depleted in the silicate Earth. While pressure increases, the correlation represented by the shaded stripes becomes steeper due to stronger binding to Fe (more negative enthalpy of

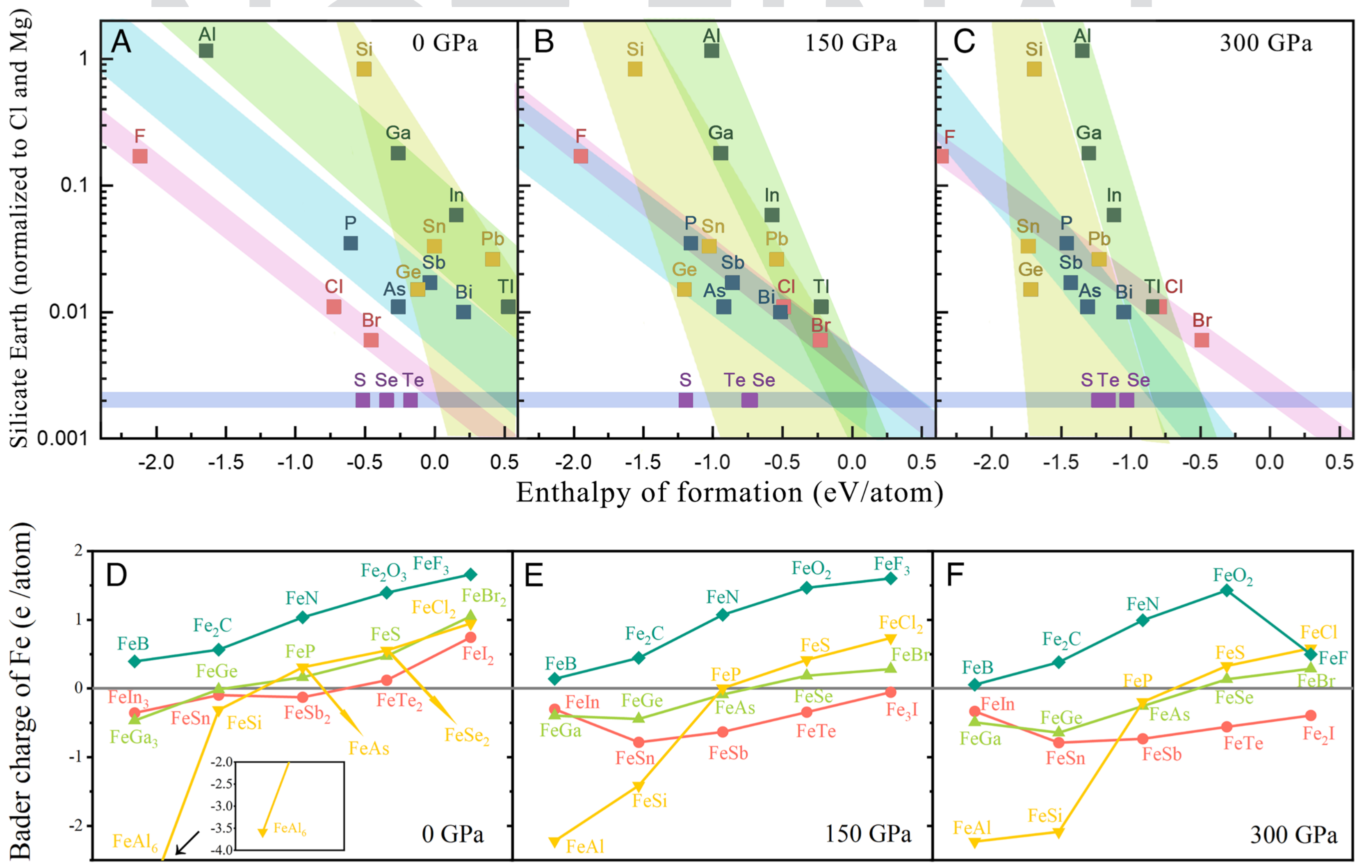

Fig. 2. Binding strength with Fe, their correlation with depletion in Earth and their chemical origin. (*A*–*C*) The correlations between element depletions and their binding strength with Fe under 0, 150, and 300 GPa. Horizontal axes show the enthalpy of formation per atom of the most stable Fe compound of selected element. The vertical axes show the abundance of an element normalized to CI chondrite and Mg. The green, yellow, blue, purple, and pink dots in the figure represent compounds formed between Fe and elements from Groups IIIA to VIIA, respectively. The corresponding shaded regions indicate the distribution of these compounds in the given coordinate space. (*D*–*F*) Calculated Bader charge of iron in Fe–*X* compounds at 0, 150, and 300 GPa.

formation) for the heavier elements such as Se, Te, Bi, and Pb. This inverse correlation clearly shows that reaction with Fe in Earth's core is unlikely to be the cause of the depletion of trace *p*-block elements in the silicate Earth, although such reactions may become exceedingly strong under terrestrial core conditions. One reason for the inverse correlations is that the volatility of an element (quantified by its condensation temperature) correlates inversely with its binding strength with Fe (i.e., the higher the volatility the weaker the binding with Fe; *SI Appendix*, Fig. S4). Another factor is that binding of an element with Fe may prevent its evaporation in primordial Earth.

Iron Redox Reversal under Pressure. To reveal the redox property of Fe, the charges of Fe in the compounds are calculated using the Quantum Theory of Atoms in Molecules method (QTAIM or Bader charge) (29, 30). The charge transfer between iron and *p*-block elements shows that, apart from Al and Si compounds (see below), the magnitude of charge transfer changes almost linearly with atomic number in each period from group 13 to group 17 (Fig. 2 *D–F*). At 0 GPa, the charge is negative for most of the *p*-block elements, indicating that iron is oxidized. The charge transfer is generally small for heavy *p*-block elements, which explains the poor stability of their Fe compounds. Generally, the charge transfer from iron to *p*-block elements decreases with increasing atomic number in the same group. For example, the Bader charges on Fe in pnictides increase in the order N > P > As > Sb. Similar increases can be found across the chalcogens and halogens. This order of increasing charge remains under increasing pressure (Fig. 2 *D–F*).

Under pressure, the electrons redistribute toward Fe, reducing its positive charge. For heavy *p*-block elements Ge, P, As, Te, and I, the charge on Fe changes from positive to negative at 0, 150, 110, 30, and 100 GPa, respectively (Fig. 2 *D–F*). This charge transfer reversal (CTR) changes the chemical character of iron from being a reductant (electron donor) at ambient pressure to an oxidant (electron acceptor) at Earth core conditions. For example, when reacted with iodine, the charge on iron changes from positive to negative at 100 GPa. In other words, iron iodide becomes iodine ferride above 100 GPa. Similar CTR also happens in Fe–B and Fe–Se compounds, but at higher pressures of 375 and 405 GPa, respectively.

We evaluate the validity of this CTR under strong correlation and magnetism effects by recalculating Bader charges using the HSE functional (*SI Appendix*, Fig. S5) and incorporating spin polarization (*SI Appendix*, Fig. S6). The results indicate that these factors have minimal impact on charge transfer. Additionally, we examine charge transfer trends using alternative charge attribution methods, particularly Mulliken and Löwdin charges (*SI Appendix*, Figs. S7 and S8). While the absolute charge values vary depending on the method and compound, all approaches consistently reveal the same overall trend in Fe chemistry under pressure. This trend confirms the occurrence of CTR and iron's transition from an electron donor to an electron acceptor under compression. Among all the charge partitioning methods, Bader charge is well suited for high-pressure studies as it is based on charge density gradients rather than projection spheres, avoiding the artifacts of sphere size and providing a more consistent approach across varying pressure conditions. Furthermore, Fig. 2 *D–F* illustrate the general trend of charge transfer in Fe compounds across different compositions. Focusing on specific compositions such as FeSi, FeP, FeI_2, and Fe_3I, the charge transfer trend becomes even more distinct, with electrons shifting back from *p*-block elements to Fe on compression (*SI Appendix*, Figs. S7 and S8). This charge redistribution mainly involves Fe *3d* and X *np* orbitals (*SI Appendix*, Fig. S9), which is the natural result of the energy shifts of the *3d* and the *np* bands (*SI Appendix*, Fig. S10). The Fe *3d* bands become lower in energy because they have a smaller radius and are therefore less prone to change under increasing pressure (*SI Appendix*, Fig. S11).

Structural Evolution of Iron Compounds. Structure evolution of Fe compounds is also affected by charge redistribution as pressure increases. At low pressure, many structures contain lone pair electrons on *p*-block elements that will disappear under high pressure, accompanying by the increase of coordination number and charge transfer back to Fe (Fig. 3 *A–D* for Fe–I; Fig. 3 *E–G* for Fe–As and Fe–Te). Both of the two stable Fe–I compounds adopt layered structures at ambient pressure, including FeI_2 in MoS_2 ($P\bar{3}m1$) and FeI_3 in $FeBr_3$ ($R\bar{3}$) structures with lone pairs on iodine anions pointing toward the space between layers (Fig. 3 *A* and *B*). However, at 150 and 300 GPa, iron-rich compounds adopt densely packed structures, including Fe_2I adopting Ni_2In structure ($P6_3/mmc$) (Fig. 3*C*) and Fe_3I adopting Cu_3Au structure ($Fm\bar{3}m$) (Fig. 3*D*). Correspondingly, the coordination number of iodine increases substantially, to 6 in Fe_2I and 12 in Fe_3I, and the lone pairs disappear, in good accordance with the CTR under pressure. Similar structure evolution is also found in other compounds containing lone pair electrons at ambient pressure, including Fe–As and Fe–Te compounds (see Fig. 3*E* for the ambient pressure phase of both $FeAs_2$ and $FeTe_2$, Fig. 3 *F* and *G*, and high-pressure phases of FeAs and FeTe, respectively). In contrast, no lone pair is found in the low-pressure structures of Fe*X* where *X* is a group 13 or 14 elements. Furthermore, some compounds contain Fe–Fe bonds in the low-pressure structure that simply vanish as pressure increases (Fig. 3*H*). For example, FeSn and FeGe are stable in a highly symmetric *P6*/*mmm* structure that contains Fe–Fe intermetallic bonds (Fig. 3*H*). While increasing pressure induces the large charge transfer to iron, Fe–Fe bonds disappear and the compounds become more ionic. At last, it is remarkable that many FeX compounds adopt the simple CsCl structure under high pressure, due to the large charge transfer to Fe. At pressures above 150 GPa, FeSn, FeGe, and FeSi transform into the CsCl structure ($Pm\bar{3}m$) (Fig. 3*I*) which is a common structure for AB type ionic compounds when the radius of A^+ and B^- ions are similar, as stated by Pauling's first rule. Complete structures and structural parameters are shown in *SI Appendix*, Fig. S12 and Table S1. Furthermore, we calculated the phonon spectra of all Fe compounds and structures, which demonstrate that they are all dynamically stable (*SI Appendix*, Figs. S13–S17).

The Silicon Anomaly. A distinctive feature emerging from our comprehensive computation of Fe chemistry is an anomaly in reacting with Si and Al. Unlike the general trend regarding the change of electron density described earlier, the charges of Fe at 0 GPa increase in the order C > Ge > Sn > Si for group 14 elements. The charges of Fe for the last three elements are very close to each other. Under pressure, the charge of Fe in Fe–Si compounds decreases most dramatically and becomes significantly lower than Ge and Sn. A similar phenomenon is apparent for group 13 elements.

This distinctive anomaly arises from the fact that the unoccupied *d* shells are significantly higher in energy for Si (and Al) and cannot host electrons, in contrast to heavier *p*-block elements, leaving large charge transfer from Si (and Al) to Fe, especially under high pressure. At 300 GPa, the charge on iron in FeSi is as low as $-2e$, indicating the very strong ionic nature of the compound. Indeed, the electron localization functions (ELF) values between Fe and Si decrease dramatically under pressure (Fig. 4 *A* and *B*). Consequently, Fe–Si bonding persistently strengthens

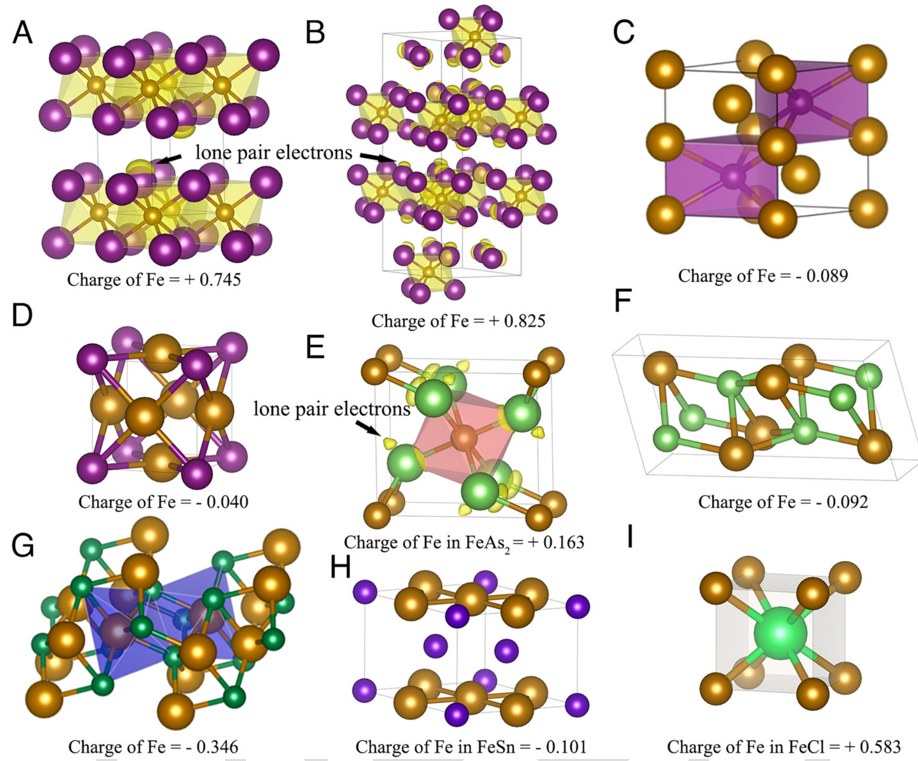

Fig. 3. Structure evolution of Fe-*p* block compounds under pressure. (*A*) Layered structure of stable FeI_2 at 0 GPa. (*B*) FeI_3 at 0 GPa; (*C*) Fe_2I at 150 GPa. (*D*) Fe_3I at 150 GPa. (*E*) FeX_2 (*X* = As and Te) structure at ambient pressure. (*F*) FeAs at 150 GPa. (*G*) FeTe at 150 GPa. (*H*) Fe*X* (*X* = Sn and Ge) with intermetallic bonds between Fe atoms. (*I*) CsCl structure, a common structure for Fe*X* compounds under pressure. Brown balls represent Fe atoms; the size (small and large) indicates the charge transfer out of or into Fe. The arrows show the interstitial space for lone pair electrons of *p*-block elements.

at increasing pressure. At 0 GPa, the Fe–Si bond strength is similar to Fe–S and Fe–P, all much weaker than Fe–O (Fig. 4*C*). With increasing pressure, the Fe–Si binding strengthens most significantly and even surpasses Fe–O at 250 GPa, implying that Si becomes siderophile at the pressure of Earth's core (31). The lower density of FeSi (*SI Appendix*, Fig. S18) under core pressures can also explain the low core density (i.e., lower than pure Fe and Ni) as revealed by seismology.

Cosmochemical analyses based on comparisons with CI chondrites alone suggest that the core's composition is approximately

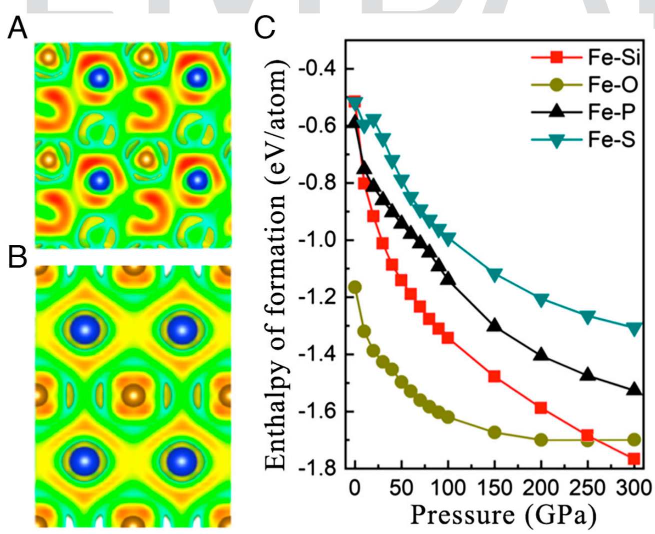

Fig. 4. Anomaly of Si in binding with Fe. ELF (32) of FeSi (*A*) at 0 GPa and (*B*) at 300 GPa. (*C*) The enthalpy of formation of Fe–X compounds as functions of pressure. The isosurfaces of the ELFs are taken at 0.2.

85 wt% Fe, 5 wt% Ni, and 1.7 wt% S (33), but the additional light element composition (e.g., Si, O, C, and H) remains largely unconstrained. The concentrations of these elements remain a subject of ongoing investigation, requiring extensive experimental, simulation, and geochemical studies. Various models estimate that the core contains approximately 5 to 8 wt.% light elements. Some suggest that S and Si are present at concentrations of 6% and 2%, respectively, aligning with geophysical data but conflicting with geochemical models that indicate sulfur's volatility (34, 35). O has been proposed as the primary contributor to the density discontinuity at the inner core boundary, while S and Si have been proposed to have minor effects (36).

Ca/Al and Mg/Si ratios are expected to exist in chondritic relative proportions in the silicate Earth, but both ratios are higher than chondritic in the shallower, accessible Earth. This suggests that either volatility controlled fractionation of Mg/Si or the presence of an Al or Si-rich domain in Earth's deep interior (37–39). Si and Al enrichment in the Earth's core may explain the higher-than-chondritic ratios in the shallower, accessible Earth.

Additionally, a comprehensive analysis of elemental distribution in Earth's interior requires comparing their chemical interactions across all compositional layers, including the silicate mantle. However, a thorough thermochemical study including crystal structure searches of all *p*-block elements reacting with silicates is currently infeasible due to computational limitations. While the present study focuses on the high-pressure chemistry of Fe, it demonstrates that increasing pressure significantly enhances the interaction of many 5*p* elements with iron due to redox reversal, strongly suggesting their incorporation into Earth's Fe core.

While silicon is predominantly found in the Earth's crust and mantle, its distribution and role in the core remain uncertain.

Earlier studies suggest that pressure has a limited effect on Si and O partitioning; however, these investigations were confined to pressures of ≤25 GPa (40–42). To account for the abundance of Si in different layers of Earth, the redox reversal and strong bonding between Si and Fe under core conditions must be considered alongside other key factors of Earth's composition, such as its bonding strength with other elements, its total abundance in Earth, and buoyancy. As the second-most abundant element, Si constitutes a major portion of the crust and mantle and bonds strongly with O. Our results do not suggest that Si transfer from the mantle to the core occurs at levels that would significantly deplete mantle Si. Instead, they support the hypothesis that Si is a key light element in the core, potentially more significant than other candidates such as H, O, and C.

Summary

We report the results of a comprehensive first-principles study of the reactivity of Fe with most of the *p*-block elements at pressures ranging from ambient to that of the center of the Earth. For each element X, the stabilities of Fe–X compounds with various stoichiometries under pressure were calculated after searching for the most stable structures using well-established algorithms and density-functional calculations. Piecing together the results for all of these compounds, we found a general trend in the chemistry of Fe under pressure—namely, Fe tends to become more electron negative and reverses its redox propensity from reductant to oxidant while reacting with many *p*-block elements at deep Earth pressures. This chemical trend is expected to have a profound effect on the distribution of elements in Earth's interior, rendering significantly enhanced of elements with Fe that is not observed near ambient pressures. Comparing the Fe binding strengths with elements that are depleted in the silicate Earth, we find a distinct inverse correlation, which strongly supports volatile depletion of these elements. On the other hand, the strong binding of light *p* elements with Fe under core conditions provides a strong chemical driving force for incorporating these elements in Earth's core. Among them, Si exhibits very strong binding with Fe under pressure, suggesting that it is a major light element component of Earth's core, i.e., lowering the seismologically constrained density of the core relative to pure Fe.

By identifying essential features of pressure-induced chemistry of Fe under deep Earth conditions, our study may be considered a necessary first step toward developing a comprehensive thermodynamically based compositional model for core. To accomplish this, other factors will need to be included. For example, the budget of light elements such as S, O, and H in the core might modify their elemental affinities for Fe under these conditions (22). However, since the Earth's core consists of predominantly Fe (and Ni), which will largely lower the activity of the light elements, the inclusion of these light elements is unlikely to overturn the chemistry of *p*-block elements in the core examined here. Furthermore, our calculations are performed for crystalline compounds and are therefore more directly related to Earth's solid inner core. On the other hand, the general trend that the chemical binding with Fe becomes much stronger under pressure can be equally applied to the liquid outer core, because the chemical driving force is expected to be similar. Furthermore, the change in Fe redox propensity under increasing pressure can also help to understand and perceive the redox state of the Earth's mantle and its evolution during the accretion of the Earth and the segregation of the core (43).

Materials and Methods

Structure Searches under Pressure. We performed structure predictions through a global minimization of free energy surfaces based on the CALYPSO (Crystal structure AnaLYsis by PSO) methodology as implemented in CALYPSO code (23, 25). We searched the structures of stoichiometric Fe_mX_n (m = 1−3; n = 1−3) with simulation cell sizes of 1 to 4 formula units under pressures of 150 GPa and 300 GPa, respectively. All the structures are optimized at a higher accuracy. In addition, the calculations for local structural relaxations and electronic properties were performed in the framework of DFT within the generalized gradient approximation Perdew–Burke–Ernzerhof (44) and frozen-core all-electron projector-augmented wave method (45, 46) as implemented in the VASP code (47). A cutoff energy of 700 eV and appropriate Monkhorst−Pack (48) k-mesh with k-points density 0.03 $Å^{-1}$ were chosen to ensure that all the enthalpy calculations were well converged to less than 1 meV/atom. The subsequent calculations also used these computational parameters.

Formation Enthalpy Calculations. For the most stable structures at each pressure, the formation enthalpy per atom is calculated using the following formula:

$$H_f(Fe_mX_n) = [H(Fe_mX_n) - mH(Fe) - nH(X)]/(m+n),$$

where H_f is the formation enthalpy per atom and H is the calculated enthalpy per chemical unit for each compound. The enthalpies for Fe and X are obtained from the most stable structures as searched by the CALYPSO method at the desired pressures. All the calculations have been performed at 0 K.

Gibbs Free Energy of Formation. We explored the effects of temperature using the QHA that introduces volume dependence of phonon frequencies as a part of anharmonic effect, for which phonon calculations were performed for all promising structures using the Phonopy code. Gibbs free energy (G) is defined at a constant temperature (T) and pressure (p) by the formula:

$$G(\mathrm{T},\ \mathrm{p}) = \min\ [\mathrm{U(V)} + F_{\mathrm{phonon}}(\mathrm{T},\ \mathrm{V}) + \mathrm{pV}],$$

where V is the volume, U is the internal lattice energy, and F_{phonon} is the phonon (Helmholtz) free energy. The minimal value for G is found at the equilibrium volume for a given T and p.

Data, Materials, and Software Availability. All study data are included in the article and/or *SI Appendix*.

ACKNOWLEDGMENTS. This work was funded by the U.S. Department of Defense (HBCU/MI W911NF2310232 to M.M.), the U.S. NSF (Nos. DMR-1848141 and OAC-2117956 to M.M.), the National Natural Science Foundation of China (No. 11974154 to X.W.), the Taishan Scholars Special Funding for Construction Projects (No. tstp20230622 to X.W.) and Special Foundation of Yantai for Leading Talents above Provincial Level (to X.W.), the Natural Science Foundation of Shandong Province (No. ZR2022MA004 to J.L.), the Academic Research Fund Tier 1 grant (RG79/23 to X.F.), the UK Natural Environment Research Council (No. NE/P012167/1 to S.A.T.R.), the Singapore Ministry of Education (MOET2EP50222-0019 to S.A.T.R.), and the U.S. DOE-NNSA (DE-NA0004153, to R.J.H.). We also thank the National Supercomputer Center Tianjin (China) for the supporting of computational resources. M.M. thanks Haiqing Lin from Beijing Computational Science Research Center for the discussion. X.W. thanks Guoliang Zhang from the Sun Yat-sen University for discussions. X.F. and S.A.T.R. thank Helen Williams from the Department of Earth Sciences, University of Cambridge, for discussions.

Author affiliations: [a]School of Physics and Electronic Information, Yantai University, Yantai 264005, China; [b]School of Materials Science and Engineering, Nanyang Technological University, Singapore 639798, Singapore; [c]Department of Chemistry and Biochemistry, California State University, Northridge, CA 91330; [d]Department of Physics, University of Illinois Chicago, Chicago, IL 60607; [e]Department of Chemistry, University of Illinois Chicago, Chicago, IL 60607; [f]Department of Earth and Environmental Sciences, University of Illinois Chicago, Chicago, IL 60607; [g]Department of Earth Science, University of California Santa Barbara, Santa Barbara, CA 93110; and [h]Asian School of the Environment, Nanyang Technological University, Singapore 639798, Singapore

Author contributions: M.M. designed research; X.W., X.F., J.L., Y.L., A.E., D.K., and M.M. performed research; X.W., X.F., J.L., A.E., S.S., A.P., R.J.H., M.J., F.S., S.R., and M.M. analyzed data; M.J., F.S., and S.R. coordinated and guided research; M.M. conceived the idea of redox reversal of Fe and designed the study; and X.W., X.F., J.L., R.J.H., M.J., F.S., S.R., and M.M. wrote the paper.

1. W. F. McDonough, S.-S. Sun, The composition of the Earth. *Chem. Geol.* **120**, 223–253 (1995).
2. D. L. Anderson, The inner inner core of Earth. *Proc. Natl. Acad. Sci. U.S.A.* **99**, 13966–13968 (2002).
3. B. J. Wood, M. J. Walter, J. Wade, Accretion of the Earth and segregation of its core. *Nature* **441**, 825 (2006).
4. E. Anders, N. Grevesse, Abundances of the elements: Meteoritic and solar. *Geochim. Cosmochim. Acta* **53**, 197–214 (1989).
5. Z. Wang, H. Becker, Ratios of S, Se and Te in the silicate Earth require a volatile-rich late veneer. *Nature* **499**, 328–331 (2013).
6. B. J. Wood, M. J. Walter, J. Wade, Accretion of the earth and segregation of its core. *Nature* **441**, 825 (2006).
7. K. Ladders, B. Fegley, *The Planetary Scientist's Companion* (Oxford University Press, New York, NY, 1998).
8. L. Zhu, H. Liu, C. J. Pickard, G. Zou, Y. Ma, Reactions of xenon with iron and nickel are predicted in the Earth's inner core. *Nat. Chem.* **6**, 644–648 (2014).
9. E. Stavrou *et al.*, Synthesis of xenon and iron-nickel intermetallic compounds at Earth's core thermodynamic conditions. *Phys. Rev. Lett.* **120**, 96001 (2018).
10. X. Du *et al.*, Structures and stability of iron halides at the Earth's mantle and core pressures: Implications for the missing halogen paradox. *ACS Earth Space Chem.* **2**, 711–719 (2018).
11. J. Liu *et al.*, Hydrogen-bearing iron peroxide and the origin of ultralow-velocity zones. *Nature* **551**, 494–497 (2017).
12. J. Liu *et al.*, Altered chemistry of oxygen and iron under deep Earth conditions. *Nat. Commun.* **10**, 153 (2019).
13. J. Botana, M.-S. Miao, Pressure-stabilized lithium caesides with caesium anions beyond the −1 state. *Nat. Commun.* **5**, 4861 (2014).
14. J. Feng, R. G. Hennig, N. W. Ashcroft, R. Hoffmann, Emergent reduction of electronic state dimensionality in dense ordered Li-Be alloys. *Nature* **451**, 445 (2008).
15. W. Zhang *et al.*, Unexpected stable stoichiometries of sodium chlorides. *Science* **342**, 1502–1505 (2013).
16. M. S. Miao, Caesium in high oxidation states and as a p-block element. *Nat. Chem.* **5**, 846–852 (2013).
17. A. R. Oganov, S. Ono, Theoretical and experimental evidence for a post-perovskite phase of MgSiO3 in Earth's D″ layer. *Nature* **430**, 445–448 (2004).
18. Q. Hu *et al.*, FeO2 and FeOOH under deep lower-mantle conditions and Earth's oxygen–hydrogen cycles. *Nature* **534**, 241–244 (2016).
19. V. A. Vernikovsky, N. V. Sobolev, The main ideas of NL Dobretsov developed by his students and teammates. *Russ. Geol. Geophys.* **57**, 3–7 (2016).
20. K. Lodders, Solar system abundances and condensation temperatures of the elements. *Astrophys. J.* **591**, 1220 (2003).
21. A. F. Goncharov *et al.*, Effect of composition, structure, and spin state on the thermal conductivity of the Earth's lower mantle. *Phys. Earth Planet. Inter.* **180**, 148–153 (2010).
22. J. Badro, A. S. Côté, J. P. Brodholt, A seismologically consistent compositional model of Earth's core. *Proc. Natl. Acad. Sci. U.S.A.* **111**, 7542–7545 (2014).
23. Y. Wang, J. Lv, L. Zhu, Y. Ma, Crystal structure prediction via particle-swarm optimization. *Phys. Rev. B* **82**, 094116 (2010).
24. A. Jain *et al.*, Commentary: The Materials Project: A materials genome approach to accelerating materials innovation. *APL Mater.* **1**, 011002 (2013).
25. Y. Wang, J. Lv, L. Zhu, Y. Ma, CALYPSO: A method for crystal structure prediction. *Comput. Phys. Commun.* **183**, 2063–2070 (2012).
26. L. V. Pourovskii *et al.*, Electronic properties and magnetism of iron at the Earth's inner core conditions. *Phys. Rev. B* **87**, 115130 (2013).
27. L. V. Pourovskii, J. Mravlje, M. Pozzo, D. Alfè, Electronic correlations and transport in iron at Earth's core conditions. *Nat. Commun.* **11**, 4105 (2020).
28. B. G. Jang, Y. He, J. H. Shim, H. Mao, D. Y. Kim, Oxygen-driven enhancement of the electron correlation in hexagonal iron at Earth's inner core conditions. *J. Phys. Chem. Lett.* **14**, 3884–3890 (2023).
29. R. F. W. Bader, Atoms in molecules. *Acc. Chem. Res.* **18**, 9–15 (1985).
30. G. Henkelman, A. Arnaldsson, H. Jónsson, A fast and robust algorithm for bader decomposition of charge density. *Comput. Mater. Sci.* **36**, 354–360 (2006).
31. J. Lin, D. L. Heinz, A. J. Campbell, J. M. Devine, G. Shen, Iron-silicon alloy in Earth's core? *Science* **295**, 313–315 (2002).
32. B. Silivi, A. Savin, Classification of chemical bonds based on topological analysis of electron locatlized functions. *Nature* **371**, 683–686 (1994).
33. K. Hirose, B. Wood, L. Vočadlo, Light elements in the Earth's core. *Nat. Rev. Earth Environ.* **2**, 645–658 (2021).
34. K. D. Litasov, A. F. Shatskiy, Composition of the Earth's core: A review. *Russ. Geol. Geophys.* **57**, 22–46 (2016).
35. G. Morard *et al.*, The Earth's core composition from high pressure density measurements of liquid iron alloys. *Earth Planet. Sci. Lett.* **373**, 169–178 (2013).
36. G. Morard, D. Andrault, D. Antonangeli, J. Bouchet, Properties of iron alloys under the Earth's core conditions. *C. R. Geosci.* **346**, 130–139 (2014).
37. M. J. Walter, E. Nakamura, R. G. Trønnes, D. J. Frost, Experimental constraints on crystallization differentiation in a deep magma ocean. *Geochim. Cosmochim. Acta* **68**, 4267–4284 (2004).
38. D. C. Rubie *et al.*, Heterogeneous accretion, composition and core–mantle differentiation of the Earth. *Earth Planet. Sci. Lett.* **301**, 31–42 (2011).
39. C. R. M. Jackson, L. B. Ziegler, H. Zhang, M. G. Jackson, D. R. Stegman, A geochemical evaluation of potential magma ocean dynamics using a parameterized model for perovskite crystallization. *Earth Planet. Sci. Lett.* **392**, 154–165 (2014).
40. U. Mann, D. J. Frost, D. C. Rubie, Evidence for high-pressure core-mantle differentiation from the metal–silicate partitioning of lithophile and weakly-siderophile elements. *Geochim. Cosmochim. Acta* **73**, 7360–7386 (2009).
41. K. Tsuno, D. J. Frost, D. C. Rubie, Simultaneous partitioning of silicon and oxygen into the Earth's core during early Earth differentiation. *Geophys. Res. Lett.* **40**, 66–71 (2013).
42. J. Wade, B. J. Wood, Core formation and the oxidation state of the Earth. *Earth Planet. Sci. Lett.* **236**, 78–95 (2005).
43. K. Armstrong, D. J. Frost, C. A. McCammon, D. C. Rubie, T. B. Ballaran, Deep magma ocean formation set the oxidation state of Earth's mantle. *Science* **365**, 903–906 (2019).
44. J. P. Perdew, K. Burke, M. Ernzerhof, Generalized gradient approximation made simple. *Phys. Rev. Lett.* **77**, 3865–3868 (1996).
45. P. E. Blöchl, Projector augmented-wave method. *Phys. Rev. B* **50**, 17953–17979 (1994).
46. G. Kresse, D. Joubert, From ultrasoft pseudopotentials to the projector augmented-wave method. *Phys. Rev. B* **59**, 1758–1775 (1999).
47. G. Kresse, J. Furthmüller, Efficient iterative schemes for ab initio total-energy calculations using a plane-wave basis set. *Phys. Rev. B* **54**, 11169–11186 (1996).
48. H. J. Monkhorst, J. D. Pack, Special points for Brillouin-zone integrations. *Phys. Rev. B* **13**, 5188–5192 (1976).

Author Query Form

Query reference	Query
Q1	Please review 1) the author affiliation and footnote symbols, 2) the order of the author names, and 3) the spelling of all author names, initials, and affiliations and confirm that they are correct as set.
Q2	Please note that the spelling of the following author names in the manuscript differs from the spelling provided in the article metadata: Matthew Jackson and Simon Redfern. The spelling provided in the manuscript has been retained; please confirm.
Q3	Please include the division or department with which the author is associated in affiliations a, b, and h.
Q4	Please review the author contribution footnote carefully. Ensure that the information is correct and that the correct author initials are listed. Note that the order of author initials matches the order of the author line per journal style. You may add contributions to the list in the footnote; however, funding may not be an author's only contribution to the work.
Q5	You have chosen to publish your PNAS article with the delayed open access option under a CC BY-NC-ND license. Your article will be freely accessible 6 months after publication, without a subscription; for additional details, please refer to the PNAS site: https://www.pnas.org/authors/fees-and-licenses. Please confirm this is correct.
Q6	Claims of priority or primacy are not allowed, per PNAS policy (https://www.pnas.org/authors/submitting-your-manuscript); therefore, the term "discovery" has been reworded. If you have concerns with this course of action, please reword the sentence or explain why the original term should not be considered a priority claim and should be reinstated.
Q7	Claims of priority or primacy are not allowed, per PNAS policy (https://www.pnas.org/authors/submitting-your-manuscript); therefore, the term "new" has been deleted. If you have concerns with this course of action, please reword the sentence or explain why the deleted term should not be considered a priority claim and should be reinstated.
Q8	Claims of priority or primacy are not allowed, per PNAS policy (https://www.pnas.org/authors/submitting-your-manuscript); therefore, the term "new" has been deleted. If you have concerns with this course of action, please reword the sentence or explain why the deleted term should not be considered a priority claim and should be reinstated.
Q9	Certain compound terms are hyphenated when used as adjectives and unhyphenated when used as nouns. This style has been applied consistently throughout where (and if) applicable.
Q10	Please check and correct the text "enhanced of elements" as intended.
Q11	Abbreviations must be used at least twice in the main text; as such GGA-PBE and PAW have been deleted.
Q12	PNAS articles should be accessible to a broad scientific audience; as such, please spell out the abbreviation VASP.
Q13	Authors are required to provide a data availability statement describing the availability or absence of all shared data (including information, code analyses, sequences, etc.), per PNAS policy (https://www.pnas.org/authors/editorial-and-journal-policies#materials-and-data-availability). As such, please indicate whether the data have been deposited in a publicly accessible database, including a direct link to the data, before your page proofs are returned. The data must be deposited BEFORE the paper can be published. Please also confirm that the data will be accessible upon publication. Note that all data deposited in a publicly accessible database (and therefore not directly available in the paper or SI) must be cited in the text with an entry in the reference list. References must include the following information: 1) author names, 2) data/page title, 3) database name, 4) a direct URL to the data, 5) the date on which the data were accessed or deposited (not the release date). For an example reference entry, visit https://www.pnas.org/author-center/submitting-your-manuscript#manuscript-formatting-guidelines. Please also indicate where the new reference citation should be added in the main text and/or data availability statement.
Q14	Abbreviations must be used at least twice in acknowledgments section; as such AcRF has been deleted.
Q15	Please confirm whether the initial "S.A.T.R." can be changed to "S.R."

Q16	If you have any changes to your Supporting Information (SI) file(s), please provide revised, ready-to-publish replacement files without annotations.
Q17	As references (9 and 18) are identical, the latter reference 18 is deleted and the subsequent references are renumbered sequentially. Please check and confirm.
Q18	Per PNAS style, all references should be numbered sequentially; hence, the references were renumbered sequentially, and their citations were updated accordingly. Please check and amend if necessary.